Sodium Dependence of Nitrofurantoin Active Transport across Mammary Epithelia and Effects of Dipyridamole, Nucleosides, and Nucleobases

Phillip M. Gerk,[1] Linda Hanson,[2] Margaret C. Neville,[2] and Patrick J. McNamara[1,3]

Received July 10, 2001; accepted November 29, 2001

Purpose. The sodium dependence and effects of nucleoside and nucleobase transport inhibitors were determined to ascertain the role of sodium dependent nucleoside or nucleobase transporters in nitrofurantoin active transport across mammary epithelia.

Methods. Five lactating female rats received steady-state intravenous infusions of nitrofurantoin with and without the broad-based inhibitor dipyridamole. In the CIT3 murine model of lactation, ^{14}C-nitrofurantoin basolateral to apical permeability was examined in the presence of varying sodium concentrations, purine and pyrimidine nucleosides and nucleobases, and dipyridamole.

Results. Dipyridamole effectively inhibited ^{14}C-nitrofurantoin flux across CIT3 cells, with K_i = 0.78 μM (95% C.I. = 0.11 to 5.3 μM) and significantly decreased the milk-to-serum ratio of nitrofurantoin from 29.2 ± 5.0 to 11.0 ± 6.3 without changing systemic clearance. Nitrofurantoin active transport was significantly inhibited by complete sodium replacement. Adenosine and guanosine significantly inhibited nitrofurantoin permeability (54.5 ± 2.6 (μl/hr)/cm^2 and 50.7 ± 0.6 (μl/hr)/cm^2, respectively, vs. control 90.5 ± 4.6 (μl/hr)/cm^2) but uridine, thymidine, and the nucleobases had no effect.

Conclusions. Nitrofurantoin active transport was sodium dependent and inhibited by dipyridamole, adenosine, and guanosine, but known sodium dependent nucleoside or nucleobase transporters were not involved.

Key words: nitrofurantoin; dipyridamole; nucleosides; nucleobases; sodium-dependence.

INTRODUCTION

In an effort to predict neonatal exposure due to the transfer of medications into breast milk, a passive diffusional model has been developed previously (1). Assuming only unbound, unionized drug crosses the mammary epithelium, this model predicts milk to serum ratios (M/S) for many medications entering milk by passive diffusion (2). However, nitrofurantoin and cimetidine are actively transported into both human and rat milk (3–6). Furthermore, nitrofurantoin, an antibiotic used to treat urinary tract infections, reaches M/S values in humans and rats of 20 and 100 times those predicted by diffusion, respectively (4–6). To make better M/S predictions, it is necessary to understand how xenobiotics such as nitrofurantoin are actively transported by the mammary gland into milk.

We observed that hypoxanthine inhibited the specific transport of nitrofurantoin across a confluent murine mammary epithelial cell (CIT3) monolayer (unpublished data). This observation suggested a role for nucleobase and/or nucleoside transport systems. Facilitative (sodium independent) and concentrative (sodium dependent) nucleoside and nucleobase transporters have been found in various epithelial and endothelial tissues of several different species (7–9). Therefore, sodium replacement and several inhibitors of nucleoside/nucleobase transport were tested for their efforts on nitrofurantoin transport in the CIT3 system.

There are several types of nucleoside transporters (7–10). The equilibrative nucleoside transporters are distinguished by their sensitivity to nitrobenzylmercaptopurine riboside (nitrobenzylthioinosine). They are both sodium independent, with a broad specificity for purines and pyrimidines, and are sensitive to 10 μM dipyridamole. Next, there are sodium-dependent secondary active nucleoside transporters, which are functionally designated N1–N6 and differ in their substrate and inhibitor selectivities, as shown in Table I (8–11). Nucleoside transporters having N1 and N2 functionality have been cloned and named CNT2 and CNT1, respectively (11). N1 and N6 prefer purine nucleosides, N2 and N4 prefer pyrimidine nucleosides, N3 accepts both, and N5 transports uridine (Table I). In contrast to N5 and N6, N1–N4 are insensitive to NBMPR (Table I). If a xenobiotic is concentrated into milk, the concentrative transporters N1–N6 would be more likely involved than the equilibrative transporters.

In regards to nucleobase transport, two equilibrative types have been identified for hypoxanthine (10). In addition, at least one Na^+ dependent nucleobase transport system has been identified, for which hypoxanthine is a substrate and guanine, uracil, and thymine are inhibitors, as shown in Table II (12–16). Furthermore, in two studies hypoxanthine transport was insensitive to 100 μM guanosine, uridine, and thymidine (12,17). Unlike the active nucleoside transporters, none of the nucleobase transporters have been cloned and functionally expressed, so functional expression systems are non-existent. Recently, nucleobase transporter-like cDNAs have been reported in humans, mice, and pigs, but so far have not been functionally expressed (18). These cDNAs may show promise as nucleobase transporters in future studies.

To examine the role of nucleoside and nucleobase transporters *in vivo* as well as *in vitro*, dipyridamole was chosen. Dipyridamole is a broadbased inhibitor of several types of nucleoside and nucleobase transporters, as well as organic cation and p-glycoprotein transporters (8,10,19,20). Also, if a sodium dependent transporter is involved, then the transport activity is expected to be sodium dependent. To determine the role of sodium dependent nucleoside or nucleobase transporters, the following algorithm was used, based on Tables I and II. If a known sodium dependent nucleoside transporter

[1] University of Kentucky College of Pharmacy, Division of Pharmaceutical Science Lexington, Kentucky 40536-0082.
[2] University of Colorado Health Science Center, Department of Physiology, Denver, Colorado 80262.
[3] To whom correspondence should be addressed. (e-mail: pmcnamar@uky.edu)

ABBREVIATIONS: M/S, milk to serum ratio; N1-N6, sodium dependent nucleoside transporters; B-A, basolateral to apical; Pe, effective permeability; J, flux; A, area; C_d, donor concentration; J_{max}, maximal flux; NS, nonspecific diffusional flux; S, substrate concentration; K_m, substrate Michaelis-Menten constant; IC_{50}, half-maximally inhibitory concentration; K_i, inhibitor Michaelis-Menten constant.

Table I. Sodium-Dependent Nucleoside Transporters

Subtype	Name	**N1**	**N2**	**N3**	**N4**	**N5**	**N6**
	designation	*cif*	*cit*	*cib*	*cit*	*cs*	*csg*
Substrates	adenosine	1–14					
(Km, μM)	guanosine	4–11		30			T
	uridine	9–40	7–13	18	4–5	T	
	thymidine	NT	5–8	13	27		
Inhibitors	adenosine	8	12–21	I, 100	I, 100	I, 1000	I, 1000
(IC50, μM)	guanosine	15	640	8–30	I, 100	I, 1000	I, 1000
	uridine	I	8–22	8–10	I, 100	I, 1000	I, 1000
	thymidine	NI	13	13–16	I, 100		NI, 1000
	NBMPR	NI	NI	NI	NI	I	0.0007
	dipyridamole	NI	NI	NI	NI	I	I, 1000
	hypoxanthine						I, 1000
	guanine						I, 1000

These data are adapted from references (8–11) where several different studies are summarized.
T indicates agent is transported, NT indicates agent is not transported.
I indicates agent is inhibitory, or NI indicates not inhibitory, and the indicated concentration (μM).
Blanks indicate undetermined data.

is involved, then both adenosine and uridine should inhibit nitrofurantoin transport, as the functionally classified N1–N6 sodium dependent nucleoside transporters are inhibited by both (8–11). If a known sodium dependent nucleobase transporter is involved, then guanine and/or uracil should inhibit nitrofurantoin transport (12–15,21).

The purpose of the present research was to determine the role of the sodium dependent nucleoside and nucleobase transporters in the active transport of nitrofurantoin across mammary epithelia by determining the effects of sodium replacement and inhibitors of nucleoside and nucleobase transporters on the process.

MATERIALS AND METHODS

Chemicals

^{14}C-nitrofurantion (58 mCi/mmol) was obtained from Chemsyn Labas (Lexena, Kansas). Polyethylene glycol 400 (PEG 400) was obtained from Union Carbide Chemical Plastic Co., Danbury, Connecticut. Organic solvents were obtained from Fisher (Pittsburgh, Pennsylvania). Cell culture reagents were obtained from Gibco BRL (Rockville, Maryland) except for hydrocortisone and insulin (Sigma, St. Louis, Missouri), epidermal growth factor (Collaborative Biomedical Products, Bedford, Massachusetts), ovine prolactin (National Hormone and Pituitary Program, Torrance, California), fetal bovine serum (Gemini Bio-Products, Calabasas, California), sterile water for injection (Baxter, McGaw Park, Illinois), and compressed gases (Scott-Gross, Lexington, Kentucky). Agents used in transport studies (Fig. 1) and all other chemicals were obtained from Sigma.

Table II. Sodium-Dependent Nucleobase Transport

	heart muscle	OK cells	LLC-PK1	renal BBMV	Choroid plexus	jejunum
hypoxanthine	8.1*	0.78*	0.79*	4.4*	31*	
guanine	6.4	0.6	5.8	1.8	I	I
thymine	5.5	4.2	3.5	7.6	I	21
uracil	7.2	3.9	2.9	30	64.6	47*
dipyridamole	30.2	0.9	4.6			

Note: This table adapted from reference (16).
Km (*) or Ki values are given in μM.
I indicates inhibitory, NI indicates not inhibitory at the indicated concentration.

In Vivo Infusions

This research adhered to the "Principles of Laboratory Animal Care" (NIH publication #85-23, revised 1985) and protocol 97-0052M was approved by the University of Kentucky Institutional Animal Care and Use Committee. In a randomized crossover study, five 300 g Sprague-Dawley lactating female rats 12–15 days post-partum were cannulated under ketamine/xylazine anesthesia. After a day to recover from surgery, the rats were randomized to receive intravenous infusions of nitrofurantoin 0.4 mg/h either with or without dipyridamole 12 mg/h. The delivery vehicle was neat polyethylene glycol 400 (0.25 ml/h) and hourly intravenous injections of 1 ml normal saline were given to prevent dehydration. Blood samples were obtained at 3, 4, and 5 h after the start of the infusion and serum was harvested by centrifugation. Milk samples were obtained at 5 h under light ketamine/xylazine anesthesia. The rats were crossed over the following day to receive the other treatment. All samples were protected from light, aliquoted, and stored frozen (–20°C) until analysis.

Serum and milk samples were extracted and analyzed by HPLC using a modified method of Pons *et. al.* (22). Briefly, furazolidone (25 μl of 5 μg/ml) was added as an internal standard to each 50 μL aliquot of serum or milk. The sample was acidified and protein precipitated by adding 100 μL of 1 N HCl and vortexing for 30 s. The sample was extracted into 1 ml methylene chloride, vortexed, and centrifuged. The organic layer was decanted, evaporated under nitrogen, and reconstituted with mobile phase. The sample was injected onto a Shimadzu (Kyoto, Japan) HPLC system with a C-18 column (Lichrosorb 5 RP18 125 × 4.0 mm, Phenomenex, Torrance California) and eluted with 10% acetonitrile 90% 25 mM potassium phosphate buffer (pH 3.00) at 1.0 ml/min. UV absorbance was measured at 366 nm. Peak height ratios (ni-

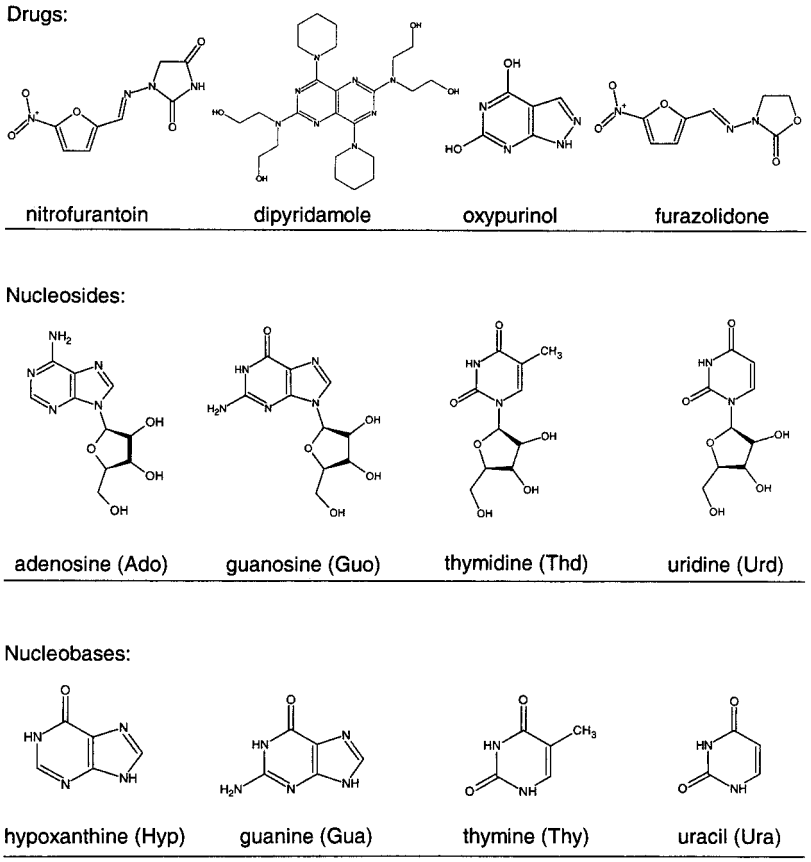

Fig. 1. Structures of agents used in transport studies. IUPAC-IUB abbreviations for nucleosides and nucleobases are in parentheses.

trofurantoin/furazolidone) were used for comparison with the standard curve.

Cell Culture Studies

CIT3 cells were cultured according to the previously published protocol (23). Briefly, the cells (passages 15 to 21) were grown in 50:50 DMEM/Ham's F12 media supplemented with 2% fetal bovine serum, epidermal growth factor (5 ng/ml), insulin (10 μg/ml), penicillin (100 U/ml), and streptomycin (100 μg/ml). The cells were seeded on #3407 Snapwell polycarbonate 0.4 μm, 1 cm^2 filter inserts (Corning-Costar, Corning, New York), then differentiated by removing epidermal growth factor and adding prolactin (3 μg/ml) and hydrocortisone (3 μg/ml).

All experiments were conducted in a buffer or medium free of antibiotics, serum, hormones, or proteins. Three types of solutions were used in the experiments. Early studies were performed in DMEM/F12 cell culture media (Gibco BRL) containing 14.3 mM $NaHCO_3$ and 10 nM HEPES at pH 7.4. Because the commercial medium contains hypoxanthine, thymidine, and other potentially interfering compounds, saline buffers were used for subsequent studies. Sodium replacement studies were conducted in Ringer's solutions containing 113 mM NaCl, 5 mM $KHCO_3$, 2 mM $CaCl_2$, 1 mM $MgSO_4$, 20 mM glucose, 10 mM HEPES, and 23 μM phenol red, pH adjusted to 7.4. NaCl was replaced with either lithium chloride or glucosamine hydrochloride. Finally, all other studies were performed with an isotonic saline buffer containing 130 mM NaCl, 4.2 mM $KHCO_3$, 1.05 mM $CaCl_{,2}$, 0.41 mM $MgSO_4$, 0.14 mM $MgCl_2$, 20 mM glucose, 10 mM HEPES, adjusted to pH = 7.4 bubbled to equilibrium with 95% oxygen 5% carbon dioxide. The calculated osmolarity was adjusted to 280-305 mOsm/L with mannitol. Humidified 95% oxygen 5% carbon dioxide was bubbled through both sides of each diffusion chamber at 20-25 ml/min, except air was bubbled in experiments where Ringer's solutions were used as above.

Before the experiments, ^{14}C-nitrofurantoin was purified by silica gel TLC (methylene chloride:acetone 3:1) and its radiochemical purity was determined by injecting an aliquot onto the HPLC system described above, sampling and counting the effluent to verify purity ⩾97%. The diffusion chambers were assembled with snapwells, filled with 5 ml on each side, and maintained at 37°C. Transepithelial resistances were measured with a Millicell meter (Millipore Corp., Bedford, Massachusetts) in each assembled diffusion chamber before, and at the end of the experiment. Resistances <300 ohm*cm^2 were cause for exclusion of that chamber. ^{14}C-Nitrofurantoin (0.4 μCi) was spiked to the basolateral side. Samples (100 μl) were obtained from the basolateral and apical chambers at 1, 20, 40, 60, 80, 100, and 120 min and were analyzed by mixing with 3a70B liquid scintillation cocktail (Research Products Inc., Mt. Prospect, Illinois) and counting on a Tri-Carb 2200CA (Packard Instrument, Meriden, Connecticut). Basolateral to apical (B-A) permeability was determined as in

Data Analysis below. Mass balance was complete, and less than 5% of the radiolabel was transferred to the opposite side in 120 min.

CIT3 Study Designs

A saturation study on the B-A permeability of nitrofurantoin was performed in DMEM/F12 using total nitrofurantoin concentrations ranging from 1 to 1600 μM. The results were fitted to the Michaelis-Menten equation by nonlinear regression (see Data Analysis).

The initial sodium dependence study was performed in Ringer's solutions isotonically replacing NaCl and LiCl or glucosamine HCl in the absence or presence of 250 μM cold nitrofurantoin and determining B-A permeability.

The first studies using adenosine, guanosine, hypoxanthine (500 μM each), and the ATP synthase inhibitor oligomycin (10 μM) were performed in DMEM/F12, comparing the B-A permeability of nitrofurantoin in control (no inhibitor) vs. treated groups. A further characterization was done with adenosine, guanosine, thymidine, uridine, hypoxanthine, guanine, thymine, uracil, and oxypurinol (100 μM each) in saline buffer. To determine the K_i value for dipyridamole, the B-A permeability of ^{14}C-nitrofurantoin was determined at dipyridamole concentrations from 0.03 μM to 100 μM (see Data Analysis).

Data Analysis

In the infusion studies, systemic clearance was determined by dividing the infusion rate by the steady-state serum concentrations. The observed milk to serum ratio (M/S) was calculated by dividing the concentration in milk by the steady state serum concentration.

In the CIT3 studies, effective permeability (Pe, (μl/h)/cm^2) was determined by calculating flux (J, pmol/hr) and dividing by the area (1 cm^2) and the donor concentration (C_d, μM) as given in Eq. (1) below. Sink conditions (no change in C_d) were assumed. GraphPad Prism v. 2.01 (GraphPad Software, Inc., San Diego, California) was used for non-linear regression. The Michaelis-Menten equation [Eq. (2)] was fitted by nonlinear regression, where J is the observed flux, J_{max} is the maximal flux, S is the concentration of nitrofurantoin, K_m is the Michaelis-Menten constant, NS is a nonspecific diffusional flux.

$$J = A * P_e * C_d \quad (1)$$

$$J = \frac{J_{max} - NS}{1 + 10^{(\log S - \log Km)}} + NS \quad (2)$$

Data from the dipyridamole inhibition experiment were fitted to Eq. (3) below to obtain $IC_{50,}$ then equation 4 was solved to obtain K_i for dipyridamole. In Eqs. (3) and (4), J is the observed flux of nitrofurantoin in the presence of dipyridamole, J_{max} is the flux of nitrofurantoin in the absence of dipyridamole, I is the concentration of dipyridamole, NS is a nonspecific diffusional flux (determined above), S is the concentration of nitrofurantoin, IC_{50} is the concentration of the inhibitor which inhibits half of the active component of the observed flux, and K_m is the Michaelis-Menten constant for nitrofurantoin transport.

$$J = \frac{J_{max} - NS}{1 + 10^{(\log I - \log IC_{50})}} + NS \quad (3)$$

$$K_i = \frac{IC_{50}}{1 + \left(\frac{S}{K_m}\right)} \quad (4)$$

Statistical Analysis

Means for M/S and systemic clearance from the rat infusion study were compared by paired *t*-tests, with $\alpha = 0.05$. Comparisons in the CIT3 determinations were made by one-way ANOVA with Dunnett's post-hoc test ($\alpha = 0.05$) using GraphPad Prism v. 2.01.

RESULTS

Results from the infusion study in lactating rats are shown in Fig. 2. Figure 2a shows that nitrofurantoin serum concentrations reached a steady-state at 3 h that was maintained through 5 h. The systemic clearance of nitrofurantoin was not changed by co-administration of dipyridamole (55.7 ± 16.6 (ml/min)/kg vs. 46.0 ± 9.1 (ml/min)/kg) (mean ± S.D.) as shown in Fig. 2b. However, dipyridamole significantly decreased the M/S of nitrofurantoin from 29.2 ± 5.0 to 11.0 ± 6.3, a 62% decrease in M/S (Fig. 2b). Both infusion regimens were well tolerated by the rats, and little or no hemolysis was observed.

Figure 3a shows the effect of increasing concentrations of cold nitrofurantoin on the flux of ^{14}C-nitrofurantoin across

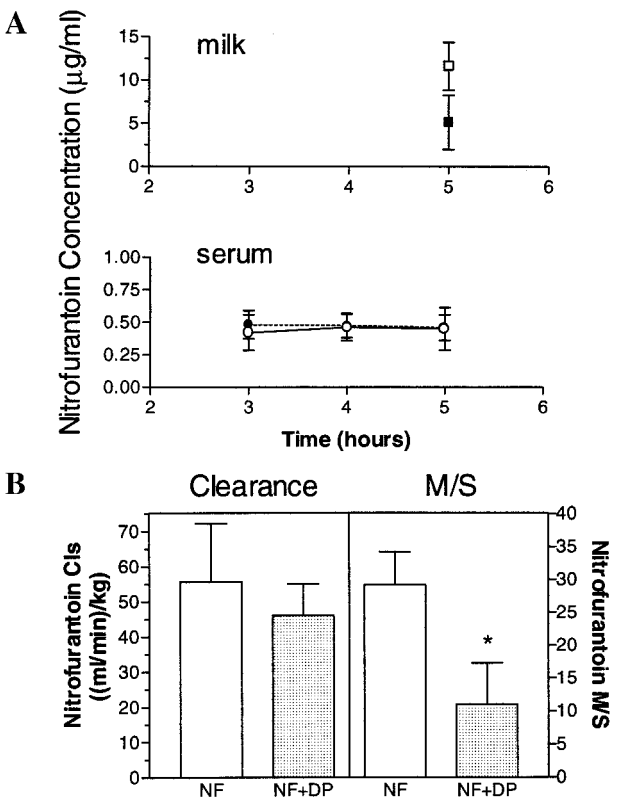

Fig. 2. Five lactating rats were infused with nitrofurantoin 0.4 mg/h alone (NF) or with dipyridamole 12 mg/h (NF+DP). Data are mean ±SD. **(A)** Milk and serum steady-state concentrations of nitrofurantoin. Milk concentrations are indicated by squares, serum concentrations are indicated by circles; filled symbols indicate the presence of dipyridamole. **(B)** Effects of dipyridamole on the M/S and systemic clearance of nitrofurantoin 0.4 mg/h. Asterisk indicates $P < 0.05$.

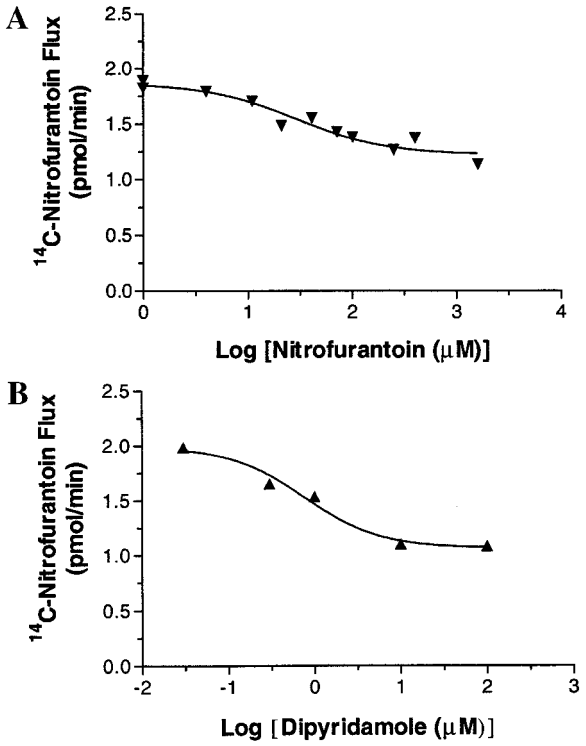

Fig. 3. Saturation and inhibition of ^{14}C-nitrofurantoin B-A flux. **(A)** Effect of cold nitrofurantoin. Regression line was fitted to equation 2. **(B)** Effect of dipyridamole on ^{14}C-nitrofurantoin B-A permeability. Regression line fitted to equation 4.

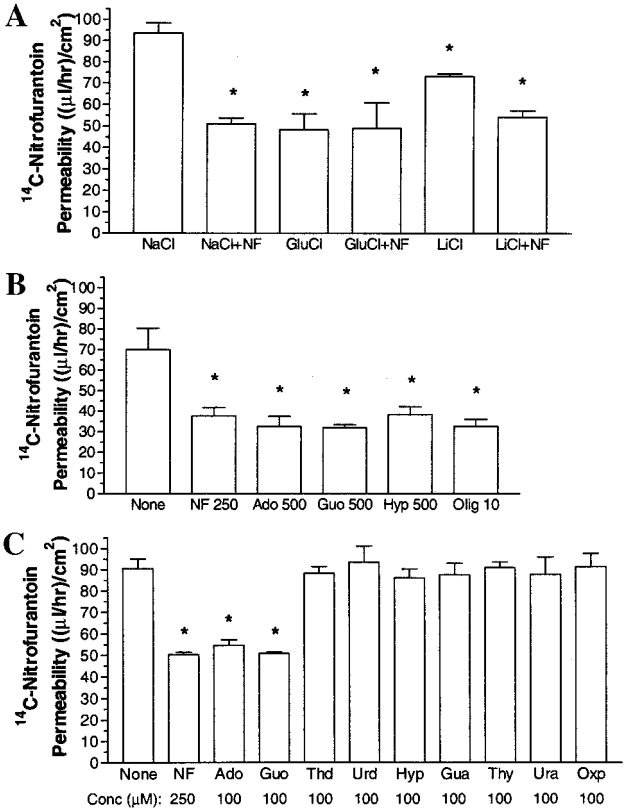

Fig. 4. Sodium dependence of ^{14}C-nitrofurantoin (1 μM) transport and effects of nucleosides and nucleobases. **(A)** Effects of sodium replacement on ^{14}C-nitrofurantoin B-A permeability. NaCl: sodium chloride Ringer's solution; +NF: 250 μM cold nitrofurantoin added to the basolateral side; LiCl: lithium chloride Ringer's solution; GluCl: glucosamine HCl Ringer's solution. Mean ± SD of 3–5 determinations. Asterisks indicate $P < 0.05$ vs. NaCl. **(B)** Effects of nitrofurantoin 250 μM (NF), adenosine 500 μM (Ado), guanosine 500 μM (Guo), hypoxanthine 500 μM (Hyp), and oligomycin 10 μM (olig) on ^{14}C-nitrofurantoin B-A permeability. Numbers indicate concentrations (μM) added to both sides, except NF added to basolateral side only. Mean ± SD of 4–8 determinations. Asterisks indicate $P < 0.05$ vs. control (none). **(C)** Effects of nucleosides and nucleobases on ^{14}C-nitrofurantoin B-A permeability. NF: 250 μM cold nitrofurantoin added to both sides; 100 μM of nucleosides or nucleobases on both sides indicated by the IUPAC-IUB abbreviations (Fig. 1); Oxp: 100 μM oxypurinol. Mean ± SD of 3–6 determinations. Asterisks indicate $P < 0.05$ vs. control (none).

CIT3 cells grown on Snapwell filters. A portion of the ^{14}C-nitrofurantoin flux was inhibitable, and therefore apparently saturable, with Km = 33.5 μM (95% CI 15.4 to 72.8 μM) as shown in Fig. 3. The observed total flux of ^{14}C-nitrofurantoin was 1.87 pmol/min (95% CI 1.75 to 1.99 pmol/min). The non-saturable flux was 1.23 pmol/min (95% CI 1.11 to 1.34 pmol/min) and the saturable component was approximately 36%. Dipyridamole effectively inhibited ^{14}C-nitrofurantoin flux across CIT3 cells, with a K_i of 0.78 μM (95% C.I. = 0.11 to 5.3 μM) as shown in Fig. 3b.

The effect on nitrofurantoin transport of complete replacement of sodium with lithium or glucosamine is shown in Fig. 4a and compared to the effect of a saturating concentration of cold nitrofurantoin (250 μM). These experiments were carried out in a modified Ringer's solution. Cold nitrofurantoin (250 μM) decreased the effective permeability of ^{14}C-nitrofurantoin from 93.6 ± 4.8 (μl/h)/cm^2 to 51.0 ± 2.7 (μl/h)/cm^2. Replacing sodium with glucosamine HCl decreased nitrofurantoin permeability to a similar value of 48.3 ± 7.3 (μl/h)/cm^2. LiCl decreased the permeability to 73.3 ± 1.4 (μl/h)/cm^2; additional inhibition was seen when cold nitrofurantoin was also added (54.3 ± 3.1 (μl/h)/cm^2), suggesting that lithium can partly substitute for sodium.

In the next experiment, we examined the effects of adenosine, guanosine, hypoxanthine and oligomycin in DMEM/F12 medium are compared with 250 μM cold nitrofurantoin (Fig. 4b). In the absence of any inhibitor, the effective permeability of ^{14}C-nitrofurantoin was 70.0 ± 10.4 (μl/h)/cm^2 but was decreased equivalently by 250 μM cold nitrofurantoin (to 37.6 ± 4.1 (μ/h)/cm^2), adenosine (to 32.4 ± 4.9 (μl/h)/cm^2), guanosine (to 31.8 ± 1.4 (μl/h)/cm^2), hypoxanthine (to 38.2 ± 3.9 (μl/h)/cm^2), and oligomycin (to 32.5 ± 3.5 (μl/h)/cm^2). A panel of nucleosides (adenosine, guanosine, thymidine, and uridine) and nucleobases (guanine, hypoxanthine, thymine, uracil, and oxypurinol) were studied in the saline (phosphate-free) buffer, shown in Fig. 4c. The control (90.5 ± 4.6 (μl/hr)/cm^2) decreased to 50.3 ± 1.1 (μl/h)/cm^2, 54.5 ± 2.6 (μl/h)/cm^2, and 50.7 ± 0.6 (μl/h)/cm^2 in the presence of nitrofurantoin, adenosine, and guanosine respectively. The pyrimidine nucleosides uridine and thymidine and the nucleobases had no significant effects.

DISCUSSION

Our studies of nitrofurantoin transport have shown an active transport component with characteristics similar but not identical to previously studied sodium dependent nucleo-

side or nucleobase transporters. In rats, we found a high M/S ratio for nitrofurantoin, which the broad-based inhibitor dipyridamole decreased by 62%. Kari *et al.* (4) reported a nitrofurantoin M/S approximately 75 times the predicted ratio for a passive process, implicating active transport into rat milk. In the rat, dipyridamole infusion (~10 mg/h) significantly inhibited incorporation of the nucleoside ^{3}H-thymidine into the bone marrow and gastrointestinal epithelium (24). The infusion rate used in our study (12 mg/h) inhibited nitrofurantoin active transport into rat milk, but did not significantly inhibit the clearance of nitrofurantoin. The involvement of a nucleoside or nucleobase transporter would be consistent with this observation in lactating rats, but other transporters can not be ruled out.

Nitrofurantoin active transport across the mammary epithelium both *in vivo* and *in vitro* was sensitive to dipyridamole (K_1 = 0.78 μM), consistent with mediation by one of several possible transporters. Dipyridamole acts as a competitive or non-competitive inhibitor of several types of transporters, and is widely used as an inhibitor or nucleoside and nucleobase transporters (8,10). Regarding the concentrative nucleoside transporters, N1–N4 are insensitive to 10 μM dipyridamole, but N5 and N6 are strongly inhibited by 10 nM and 20 μM dipyridamole, respectively (10,25,26), although the type of inhibition has not been determined for either one. Sundaram *et al.* reported that dipyridamole competitively inhibits the human equilibrative nucleoside transporter hENT1 with an IC50 of 198 ± 24 nM and a Hill coefficient of 1.25 ± 0.12, suggesting that one molecule binds to the binding site (27). Furthermore, chimeras they constructed of hENT1 with rENT1 (insensitive to dipyridamole) demonstrate that the inhibition is linked to specific domains of the protein (27).

Dipyridamole was shown to inhibit several other types of transporters. It was reported to inhibit organic cation transporters, although the type of inhibition was not reported (19). Bendayan *et al.* demonstrated that 50 μM dipyridamole inhibited uptake of the organic cation n-methylnicotinamide, and that dipyridamole had an IC_{50} of 7.7 μM against cimetidine uptake by LLC-PK1 cells (19). Dipyridamole inhibited p-glycoprotein (28); furthermore, Ayesh *et al.* showed that dipyridamole competed with verapamil for binding to p-glycoprotein, with a Hill coefficient of 2 (20). Additionally, it exerted a mixed competitive/non-competitive inhibition of bicarbonate-chloride exchange, with an IC_{50} of 4μM (29). Plagemann and Woffendin showed that dipyridamole inhibited 2-deoxy-D-glucose transport without changing the transition temperature of the transporter (30). Although dipyridamole is quite lipophilic (logD = 2.2 at pH 7.4; from ACD/LogP DB v4.0 using ACD/I-Lab service), this finding suggests that the inhibition of glucose transport by dipyridamole is not mediated by an alteration in membrane fluidity (30). The consensus amongst these studies is that although dipyridamole is a broad-based inhibitor of various transporters, the inhibition is due to binding of the drug to the various transport proteins rather than to changes in the properties of the membrane.

Toddywalla *et al.* reported a Ki of 53 ± 41 μM for nitrofurantoin transport across CIT3 cells grown on Snapwell filters, while performing the experiments in DMEM/F12 (23). In the present study we determined a Km of similar magnitude, 33.5 μM (95% Cl 15.4 to 72.8 μM), for nitrofurantoin transport in saline buffer. Toddywalla *et al.* also reported a B-A nitrofurantoin permeability of 64 ± 5 × 10^{-3} cm/h (or (μl/h)/cm^2) of which approximately 40% was inhibited by high nitrofurantoin concentrations (23). Similarly, in this study we observed a nitrofurantoin B-A permeability of 70 (μl/h)/cm^2 in DMEM/F12, 47% of which was inhibitable. For experiments in Ringer's solution or the saline buffer, the B-A permeability ranged from 74.5 to 97.4 (μl/h)/cm^2, 35.7% to 51.5% of which was inhibitable. Because DMEM/F12 contains sodium and many potentially interacting substances (e.g., hypoxanthine, thymidine, phenol red, amino acids, and vitamins), other buffers were required for characterization studies. The Ringer's solution was chosen initially to conveniently replace sodium. However, the salt concentrations are different from the concentrations in the media in which the cells are cultured. The saline buffer (described above in Methods) was designed to provide similar concentrations of the major salt components, but without phosphates.

Sodium dependence was demonstrated in this study. Also, inhibition of active transport by the ATP synthase inhibitor oligomycin is consistent with an energy dependent process. Furthermore, lithium substitution only partially decreased nitrofurantoin B-A permeability, suggesting lithium may have substituted for sodium to some extent. By contrast, the nucleoside transporters generally show very high sodium specificity (10).

As mentioned previously, if the functionally classified N1–N6 sodium dependent nucleoside transporters were involved, then both adenosine and uridine should have inhibited nitrofurantoin transport (8–11). Because the Km's for these agents range from 1–45 μM (8,10), the 100 μM concentrations used in this study would inhibit the nucleoside transporters by >50%. However, this study showed that adenosine but not uridine inhibited nitrofurantoin transport. These results are not consistent with the known nucleoside transporters. Furthermore, guanosine but not thymidine inhibited transport, suggesting a preference for purine nucleosides.

If a known sodium dependent nucleobase transporter were involved, then guanine and/or uracil should inhibit nitrofurantoin transport (12–15,21). The Ki's for guanine and uracil inhibition of hypoxanthine transport range 0.6–6.4 μM and 2.9–64.6 μM, respectively (12–15,17). Furthermore, the Km for hypoxanthine transport range is 0.78–31.1 μM (14,15). At the concentrations used in this study, a nucleobase transporter similar to those previously reported would be inhibited by approximately 50% or more. Although hypoxanthine was inhibitory at 500 μM, neither hypoxanthine nor the other nucleobases were inhibitory at 100 μM. This finding is not predicted from the previously characterized sodium dependent nucleobase transport systems.

CONCLUSIONS

Dipyridamole effectively inhibited the active transport of nitrofurantoin across mammary epithelia both *in vitro* with a high affinity and *in vivo.* Nitrofurantoin transport across the CIT3 model was sodium dependent. The effects of nucleosides and nucleobases on nitrofurantoin transport are not consistent with other studies on functionally classified nucleoside and nucleobase transporters. These results suggest that nitrofurantoin does not interact with the previously characterized nucleoside or nucleobase transporters. Further *in vivo, in vitro,* and molecular studies are required to elucidate the specific transport system for nitrofurantoin in mammary

epithelia. Understanding these mechanisms will allow better M/S predictions to be made, aiding clinicians to better assess the inadvertant exposure of suckling infants to various agents.

ACKNOWLEDGMENTS

This project was supported by the University of Kentucky Medical Center through the Women's Health Initiative. PMG was supported by the University of Kentucky Research Challenge Trust Fund, Dissertation Enhancement Award, and the Peter Glavinos Travel Award.

REFERENCES

1. J. C. Fleishaker, N. Desai, and P. J. McNamara. Factors affecting the milk-to-plasma drug concentration ratio in lactating women: physical interactions with protein and fat. *J. Pharm. Sci.* **76:**189–193 (1987).
2. J. C. Fleishaker and P. J. McNamara. *In vivo* evaluation in the lactating rabbit of a model for xenobiotic distribution into breast milk. *J. Pharmacol. Exp. Ther.* **244:**919–924 (1988).
3. C. Y. Oo, R. J. Kuhn, N. Desai, and P. J. McNamara. Active transport of cimetidine into human milk. *Clin. Pharmacol. Ther.* **58:**548–555 (1995).
4. F. W. Kari, R. Weaver, and M. C. Neville. Active transport of nitrofurantoin across the mammary epithelium in vivo. *J. Pharmacol. Exp. Ther.* **280:** 664–668 (1997).
5. P. J. McNamara, J. A. Meece, and E. Paxton. Active transport of cimetidine and ranitidine into the milk of Sprague Dawley rats. *J. Pharmacol. Exp. Ther.* **277:**1615–1621 (1996).
6. P. M. Gerk, R. J. Kuhn, N. Desai, and P. J. McNamara. Active transport of nitrofurantoin into human milk. *Pharmacotherapy* **21:**669–675 (2001).
7. J. A. Belt, N. M. Marina, D. A. Phelps, and C. R. Crawford. Nucleoside transport in normal and neoplastic cells. *Adv. Enzyme Regul.* **33:**235–252 (1993).
8. J. A. Thorn and S. M. Jarvis. Adenosine transporters. *Gen. Pharmacol.* **27:**613–620 (1996).
9. J. Wang, M. E. Schaner, S. Thomassen, S.-F. Su, M. Piquette-Miller, and K. M. Giacomini. Functional and molecular characteristics of Na^+-dependent nucleoside transporters. *Pharm. Res.* **14:**1524–1532 (1997).
10. D. A. Griffith and S. M. Jarvis. Nucleoside and nucleobase transport systems of mammalian cells. *Biochim. Biophys. Acta* **1286:**153–181 (1996).
11. C. E. Cass, J. D. Young, and S. A. Baldwin. Recent advances in the molecular biology of nucleoside transporters of mammalian cells. *Biochem. Cell Biol.* **76:**761–770 (1998).
12. D. A. Griffith and S. M. Jarvis. High affinity sodium-dependent nucleobase transport in cultured renal epithelial cells (LLC-PK1). *J. Biol. Chem.* **268:**20085–20090 (1993).
13. D. A. Griffith and S. M. Jarvis. Characterization of a sodium-dependent concentrative nucleobase-transport system in guinea-pig kidney cortex brush-border membrane vesicles. *Biochem. J.* **303:**901–905 (1994).
14. M. Shayeghi, R. Akerman, and S. M. Jarvis. Nucleobase transport in opossum kidney epithelial cells and Xenopus laevis oocytes: the characterization, structure-activity relationship and -independent hypoxanthine uptake. *Biochim. Biophys. Acta* **1416:** 109–118 (1999).
15. C. B. Washington and K. M. Giacomini. Mechanisms of nucleobase transport in rabbit choroid plexus. Evidence for a Na(+)-dependent nucleobase transporter with broad substrate selectivity. *J. Biol. Chem.* **270:**22816–22819 (1995).
16. H. de Koning and G. Diallinas. Nucleobase transporters (review). *Mol. Membr. Biol.* **17:**75–94 (2000).
17. P. S. Haddock. Evidence for sodium-dependent hypoxanthine uptake in isolated guinea pig ventricular myocytes: stimulation by extracellular N_i^{2+}. *Cardiovasc. Res.* **30:**130–137 (1995).
18. C. Faaland, J. Race, G. Ricken, F. Warner, W. Williams, and E. Holtzman. Molecular characterization of two novel transporters from human and mouse kidney and from LLC-PK1 cells reveals a novel conserved family that is homologous to bacterial and Aspergillus nucleobase transporters. *Biochim. Biophys. Acta* **1442:**353–360 (1998).
19. R. Bendayan. Interaction of dipyridamole, a nucleotide transport inhibitor, with the renal transport of organic cations by LLCPK1 cells. *Can. J. Physiol. Pharmacol.* **75:**52–56 (1997).
20. S. Ayesh, Y. M. Shao, and W. D. Stein. Co-operative, competitive and non-competitive interactions between modulators of P-glycoprotein. *Biochim. Biophys. Acta* **1316:**8–18 (1996).
21. J. R. Bronk and J. G. Hastewell. The transport of pyrimidines into tissue rings cut from rat small intestine. *J. Physiol.* **382:**475–488 (1987).
22. G. Pons, E. Rey, M.-O. Richard, F. Vauzelle, C. Francoual, C. Moran, P. d'Athis, J. Badoual, and G. Olive. Nitrofurantoin excretion in human milk. *Dev. Pharmacol. Ther.* **14:**148–152 (1990).
23. V. S. Toddywalla, F. W. Kari, and M. C. Neville. Active transport of nitrofurantoin across a mouse mammary epithelial monolayer. *J. Pharmacol. Exp. Ther.* **280:**669–676 (1997).
24. D. R. Newell, P. M. O'Connor, A. H. Calvert, and K. R. Harrap. The effect of the nucleoside transport inhibitor dipyridamole on the incorporation of [3H]thymidine in the rat. *Biochem. Pharmacol.* **35:**3871–3877 (1986).
25. S. D. Patil and J. D. Unadkat. Sodium-dependent nucleoside transport in the human intestinal brush-border membrane. *Am. J. Physiol.* **272:**G1314–1320 (1997).
26. S. A. Flanagan and K. A. Mecklin-Gill. Characterization of a novel Na+-dependent, guanosine-specific, nitrobenzylthioinosine-sensitive transporter in acute promyelocytic leukemia cells. *J. Biol. Chem.* **272:**18026–18032 (1997).
27. M. Sundaram, S. Y. Yao, A. M. Ng, M. Griffiths, C. E. Cass, S. A. Baldwin, and J. D. Young. Chimeric constructs between human and rat equilibrative nucleoside transporters (hENT1 and rENT1) reveal hENT1 structural domains interacting with coronary vasoactive drugs. *J. Biol. Chem.* **273:**21519–21525 (1998).
28. E. Hosoi, M. Hirose, S. Hamano, M. Morimoto, and Y. Kuroda. Effect of MDR antagonists on the cidal activity of vincristine for cells expressing MDR-1 is superior to those expressing MRP. *Int. J. Oncol.* **13:**343–348 (1998).
29. T. Heming, C. Vanoye, and A. Bidani. Dipyridamole inhibition of HCO_3-Cl^- exchange in human erythrocytes. *J. Pharmacol. Exp. Ther.* **255:**631–635 (1990).
30. P. G. Plagemann and C. Woffendin. Comparison of the equilibrium exchange of nucleosides and 3-O-methylglucose in human erythrocytes and of the effects of cytochalasin B, phloretin and dipyridamole on their transport. *Biochim. Biophys. Acta* **899:**295–301 (1987).